

# A Fluorinated Detergent for Membrane-Protein Applications\*\*

Erik Frotscher, Bartholomäus Danielczak, Carolyn Vargas, Annette Meister, Grégory Durand, and Sandro Keller\*

**Abstract:** Surfactants carrying fluorocarbon chains hold great promise as gentle alternatives to conventional hydrocarbon-based detergents for the solubilization and handling of integral membrane proteins. However, their inertness towards lipid bilayer membranes has limited the usefulness of fluorinated surfactants in situations where detergent-like activity is required. We demonstrate that fluorination does not necessarily preclude detergency, as exemplified by a fluorinated octyl maltoside derivative termed F<sub>6</sub>OM. This nonionic compound readily interacts with and completely solubilizes phospholipid vesicles in a manner reminiscent of conventional detergents without, however, compromising membrane order at subsolubilizing concentrations. Owing to this mild and unusual mode of detergency, F<sub>6</sub>OM outperforms a lipophobic fluorinated surfactant in chaperoning the functional refolding of an integral membrane enzyme by promoting bilayer insertion in the absence of micelles.

Most in vitro approaches to handling membrane proteins rely on detergents, that is, surface-active compounds that interact with and, at sufficiently high concentrations, disrupt lipid bilayer membranes.<sup>[1]</sup> Detergent-solubilized proteins can then be purified and subjected to biochemical, biophysical, or structural scrutiny<sup>[2]</sup> or reconstituted into artificial bilayers.<sup>[3,4]</sup>

However, exposure to detergents often results in the irreversible loss of native protein structure and function owing to the disruption of stabilizing interactions within the protein or with lipids.<sup>[5,6]</sup> Recent years have witnessed increasing efforts at developing new amphiphiles that could substitute for conventional detergents in solubilizing membrane proteins without compromising their integrity.<sup>[7]</sup> Notable examples include lipid nanodiscs bounded by scaffold proteins<sup>[8]</sup> or styrene maleic acid copolymers,<sup>[9]</sup> amphiphilic polymers known as amphipols,<sup>[10]</sup> tripod amphiphiles,<sup>[11]</sup> and fluorinated surfactants.<sup>[12–14]</sup> The latter retain the most favorable properties of hydrocarbon-based detergents but overcome many of their limitations.<sup>[7]</sup> By analogy to the poor miscibility of liquid hydrocarbons and fluorocarbons, contacts between fluorinated surfactant tails and hydrocarbon moieties of proteins and lipids are expected to be unfavorable, such that structurally or functionally important protein/protein and protein/lipid interactions are not disrupted.<sup>[12,13]</sup> Moreover, fluorocarbon chains are bulkier than their hydrocarbon counterparts, which prevents them from intruding between protein transmembrane domains.<sup>[7,12]</sup>

The peculiarity of fluorocarbon chains of being both hydrophobic and lipophobic is thought not only to prevent protein denaturation and delipidation but also to render fluorinated surfactants poor solubilizers<sup>[13–18]</sup> unless they contain a harsh, ionic headgroup.<sup>[19]</sup> Herein, we show that, contrary to this assumption, nonionic fluorinated surfactants can be powerful yet mild detergents. Comparison of two compounds sharing the same fluorocarbon chain but different headgroups reveals that fluorination does not necessarily guarantee lipophobicity. Instead, it is the properties of the polar headgroup that, in conjunction with a fluorocarbon chain, govern the detergency, or lack thereof, of fluorinated surfactants. While this calls for caution when employing fluorinated surfactants in experiments where membrane integrity is essential,<sup>[20–22]</sup> it also paves the way for their judicious use in biochemical approaches requiring detergent activity without the need for conventional hydrocarbon-based detergents.

We first compared the self-assembly and membrane solubilization properties of 3,3,4,4,5,5,6,6,7,7,8,8,8-tridecafluoro-*n*-octyl- $\beta$ -D-maltopyranoside (F<sub>6</sub>OM) and 3,3,4,4,5,5,6,6,7,7,8,8,8-tridecafluoro-*n*-octylphosphocholine (F<sub>6</sub>OPC), both of which carry an octyl chain with a perfluorinated terminal hexyl segment (Figure 1). Nonionic F<sub>6</sub>OM self-assembled into elongated rod-shaped micelles observable by transmission electron microscopy (Figure 2a), whereas zwitterionic F<sub>6</sub>OPC micelles appeared smaller and spheroidal, as judged by dynamic light scattering (Figure S1 in the Supporting Information). This contrasts with an F<sub>6</sub>OPC analogue bearing two more CF<sub>2</sub> groups, which forms bilayer mem-

[\*] E. Frotscher, B. Danielczak, Dr. C. Vargas, Prof. S. Keller  
Molecular Biophysics, University of Kaiserslautern  
Erwin-Schrödinger-Str. 13, 67663 Kaiserslautern (Germany)  
E-mail: mail@sandrokeller.com

Priv.-Doz. A. Meister  
Center for Structure and Dynamics of Proteins (MZP)  
Martin Luther University Halle-Wittenberg  
Biocenter, Weinbergweg 22, 06120 Halle, Saale (Germany)

Dr. G. Durand  
Equipe Chimie Bioorganique et Systèmes Amphiphiles  
Université d'Avignon et des Pays de Vaucluse  
33 rue Louis Pasteur, 84000 Avignon (France)  
and  
Institut des Biomolécules Max Mousseron  
UMR 5247 CNRS-UM-ENSCM  
15 avenue Charles Flahault, 34093 Montpellier Cedex 05 (France)

[\*\*] We are indebted to Prof. Dr. Heiko Heerklotz and Sara Hovakeemian (both University of Toronto) and to Dr. Harald Kelm (University of Kaiserslautern) for providing access to and help with time-resolved fluorescence and NMR spectroscopy, respectively. We thank Markus Fleisch, Michaela Herrmann, Jessica Klement, and Sebastian Unger (University of Kaiserslautern) for excellent experimental assistance. This work was partly funded by the Deutsche Akademische Austauschdienst (DAAD) with grant no. 56041134 to SK and by the Deutsche Forschungsgemeinschaft (DFG) through International Research Training Group (IRTG) 1830.

Supporting information for this article is available on the WWW under <http://dx.doi.org/10.1002/anie.201412359>.

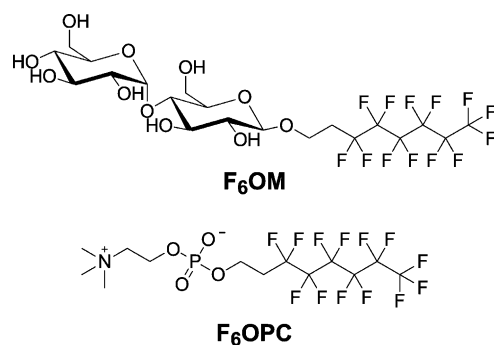


**Figure 1.** Chemical structures of F<sub>6</sub>OM and F<sub>6</sub>OPC.

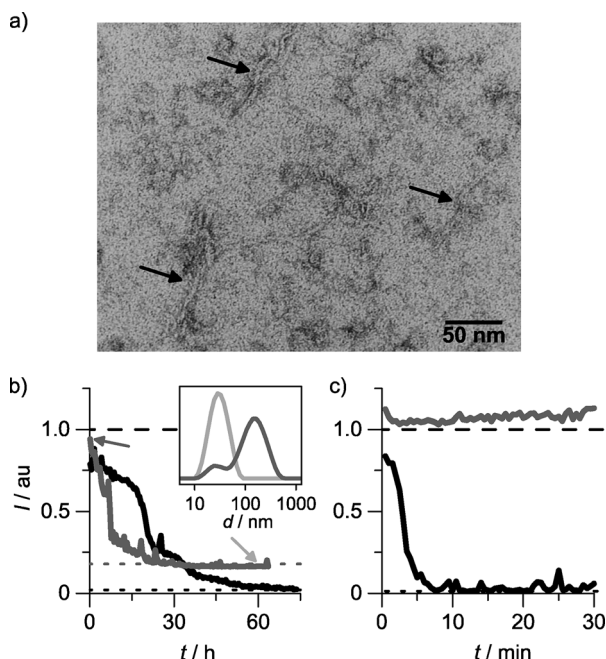


**Figure 2.** Differential solubilization of lipid vesicles by fluorinated surfactants. a) Negative-stain transmission electron micrograph of 1 mM F<sub>6</sub>OM. Arrows indicate rod-shaped micelles. b) Kinetics of vesicle solubilization by F<sub>6</sub>OM at 25°C as reflected in 90° light scattering intensity *I* as a function of time *t*. 0.1 mM POPC in the form of LUVs was incubated with 2 mM (black) or 10 mM (gray) F<sub>6</sub>OM. Horizontal lines represent mean intensities for pure POPC LUVs (dashed line) or pure F<sub>6</sub>OM micelles (dotted lines) at the respective concentrations. Inset: Intensity-weighted particle size distributions obtained immediately (gray) or 60 h (light gray) after mixing 0.1 mM POPC LUVs with 10 mM F<sub>6</sub>OM (see arrows in main panel). c) Solubilization kinetics at 60°C as reflected by *I* as a function of *t*. 0.1 mM POPC LUVs were mixed with 2 mM F<sub>6</sub>OM (black) or 20 mM F<sub>6</sub>OPC (gray).

branes.<sup>[23]</sup> Under the conditions used in our experiments, the critical micellar concentrations (CMCs) of F<sub>6</sub>OM and F<sub>6</sub>OPC were 0.7 mM and 2.9 mM, respectively, as determined by calorimetric demicellization titrations<sup>[24]</sup> (Figure S2) and confirmed by <sup>19</sup>F NMR spectroscopy<sup>[16]</sup> (Figure S3). At 25°C, exposure of large unilamellar vesicles (LUVs) composed of the phospholipid 1-palmitoyl-2-oleyl-*sn*-glycero-3-phosphocholine (POPC) to micellar F<sub>6</sub>OM resulted in slow

but steady solubilization, as indicated by a decrease in light scattering intensity (Figure 2b). Solubilization of 0.1 mM POPC LUVs required several days at 2 mM F<sub>6</sub>OM and 25°C but was greatly accelerated by increasing the surfactant concentration to 10 mM (Figure 2b) or raising the temperature to 60°C (Figure 2c). By contrast, F<sub>6</sub>OPC did not affect vesicle integrity even at 60°C and a concentration of 20 mM (Figure 2c), in agreement with the poor performance of longer-chain analogues as membrane solubilizers.<sup>[15]</sup> These differences in solubilizing power rationalize the observation that F<sub>6</sub>OPC but not F<sub>6</sub>OM is compatible with free-standing lipid bilayers.<sup>[20]</sup>

A systematic study of the solubilization behavior and the supramolecular organization of POPC/F<sub>6</sub>OM mixtures was carried out by recording the intensity of scattered light as a function of the concentrations of both components<sup>[25]</sup> (Figure 3a). The F<sub>6</sub>OM concentrations required for initiating and completing solubilization increased linearly with POPC concentration, thus allowing the construction of a phase diagram<sup>[26]</sup> in which a coexistence range separates two regions where either only bilayer or only micellar structures exist (Figure 3b). As derived from the slopes of the phase boundaries, solubilization starts when the molar F<sub>6</sub>OM/POPC ratio in the membrane reaches 1.0 and is completed at a molar ratio of 3.0 in the mixed micelles. From this, we determined the free-energy costs of transferring POPC into micelles or F<sub>6</sub>OM into bilayers to be as low as 1.7 kJ mol<sup>−1</sup> and 1.0 kJ mol<sup>−1</sup>, respectively. These values fall close to those observed for typical detergents (Table S1 in the Supporting Information) but are very different from the characteristics of a “membranophobic” lipopeptide.<sup>[27]</sup> <sup>31</sup>P and <sup>19</sup>F NMR experiments confirmed the concomitant transfer of POPC and F<sub>6</sub>OM from bilayers into micelles. The <sup>31</sup>P signal was broadened beyond detection in vesicular POPC suspensions because of the slow tumbling of LUVs,<sup>[28]</sup> but a sharp isotropic peak appeared upon solubilization by F<sub>6</sub>OM and remained constant after complete transfer of POPC into micelles (Figure 3c,e). In <sup>19</sup>F NMR spectra,<sup>[16]</sup> the onset of solubilization manifested as an upfield shift in the signal from the CF<sub>3</sub> group of F<sub>6</sub>OM, which continued to change upon variation of the composition of the mixed micelles through further addition of F<sub>6</sub>OM (Figure 3d,e).

Fast vesicle solubilization at elevated temperatures has been ascribed to thermally induced membrane destabilization and accelerated detergent translocation.<sup>[25,29]</sup> We carried out uptake and release assays by isothermal titration calorimetry<sup>[30]</sup> to test this hypothesis for F<sub>6</sub>OM and dissect the thermodynamics of its interactions with lipid membranes (Figure 4a,c). Analysis of the resulting isotherms (Figure 4b,d) in terms of a membrane/water partition equilibrium<sup>[30]</sup> revealed that F<sub>6</sub>OM strongly partitioned into POPC membranes, with transfer free energies of −25.3 kJ mol<sup>−1</sup> at 25°C and −29.0 kJ mol<sup>−1</sup> at 60°C (Table S2), and that the accessible lipid fraction dramatically increased with temperature (Table S3). This indicates that F<sub>6</sub>OM readily translocates between the two bilayer leaflets at 60°C but not at 25°C and that this difference is responsible for the temperature dependence of its solubilization kinetics (Figure 2b,c). By contrast, titration of F<sub>6</sub>OPC produced only minute heats of

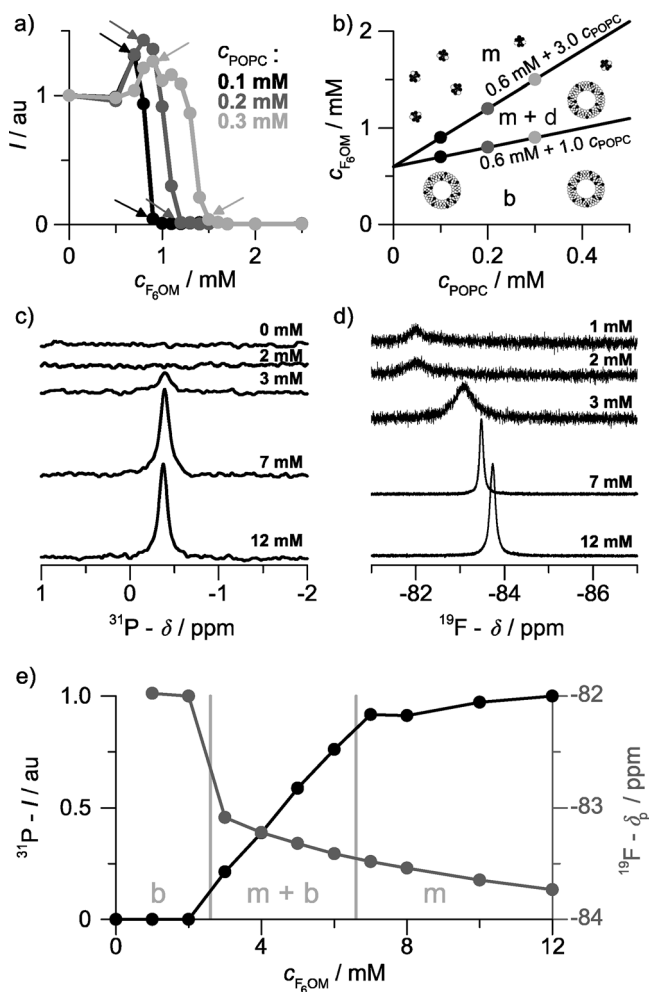


**Figure 3.** Solubilization of POPC vesicles as a function of  $F_6OM$  concentration. a)  $90^\circ$  light scattering intensity  $I$  during solubilization in which POPC LUVs were challenged with increasing concentrations of  $F_6OM$ . Arrows indicate data points used for constructing the phase diagram. b) POPC/ $F_6OM$  phase diagram showing ranges in which only bilayers (b), only micelles (m), or both (m + b) exist. Phase boundaries (solid lines with fitting parameters) are linear fits to concentration pairs (circles) taken from part (a). c)  $^{31}P$  NMR spectra for 2 mM POPC LUVs mixed with the indicated concentrations of  $F_6OM$  in 90%  $H_2O$ /10%  $D_2O$ . d)  $^{19}F$  NMR spectra for the same samples focusing on the  $CF_3$  resonance of  $F_6OM$ . For clarity, vertical scaling is non-uniform across different  $F_6OM$  concentrations. e)  $^{31}P$  NMR peak intensities ( $I$ ; black) and  $^{19}F$  NMR peak chemical shifts ( $\delta_p$ ; gray) of the  $CF_3$  group against  $F_6OM$  concentration. Gray lines indicate phase boundaries predicted by the phase diagram in (b). Each sample was incubated at  $60^\circ C$  for 30 min to ensure equilibration before measurements were performed at  $25^\circ C$ .

dilution (data not shown), thus suggesting the absence of notable interactions with POPC membranes.

We measured time-resolved fluorescence anisotropy<sup>[31]</sup> to shed more light on the mechanism of  $F_6OM$ -driven membrane solubilization. Titration of phospholipid membranes with detergents containing a polar headgroup and a hydrophobic tail results in a progressive increase in acyl chain disorder, as reflected in changes in the nanosecond dynamics of the fluorescent probe 1,6-diphenyl-1,3,5-hexatriene (DPH).<sup>[32]</sup> At  $20^\circ C$ , POPC bilayers start disintegrating when

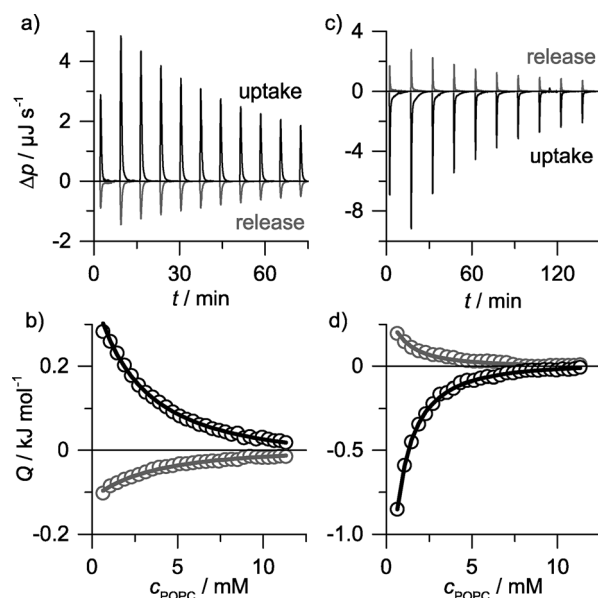


**Figure 4.** Membrane partitioning and translocation of  $F_6OM$  by ITC. a) Uptake and release thermograms at  $25^\circ C$  depicting differential heating power  $\Delta p$  versus time  $t$ . For clarity, only 11 of 30 injections are shown. b) Corresponding isotherms illustrating experimental (circles) and fitted (solid lines) values for the integrated and normalized heat of reaction  $Q$ , yielding an accessible POPC fraction of 0.22. c) Uptake and release thermograms at  $60^\circ C$ . Only 10 of 30 injections are shown. d) Corresponding isotherms of experimental (circles) and fitted (solid lines)  $Q$  values, resulting in an accessible POPC fraction of 0.65. The POPC concentration in the injection syringe was always 60 mM, while the  $F_6OM$  concentration was 0.3 mM in the cell for uptake titrations and 3 mM in the syringe for release titrations. These concentrations ensured that only bilayers and no micelles were present.

the limiting anisotropy of DPH decreases to a threshold of approximately 0.01, irrespective of the chemical nature of the detergent.<sup>[33]</sup> In contrast with this “homogeneous” solubilization mechanism, some detergent-like lipopeptides and detergents with polar and nonpolar moieties that are not clearly segregated solubilize membranes “heterogeneously”, that is, they cluster together within the lipid matrix and induce solubilization without significantly affecting the overall membrane order.<sup>[33]</sup> The latter mode of solubilization was also observed for  $F_6OM$ , which induced only minor changes before solubilization set in (Figure 5). Upon further addition of  $F_6OM$ , the limiting anisotropy rose steadily and finally plateaued when solubilization was complete. The decreased ability of micelle-solubilized DPH to reorient is in agreement with a rod-shaped micellar morphology (Figure 2a) and thus a large apparent hydrodynamic diameter (Figure S1). Lipophobic  $F_6OPC$  had no effect on POPC membranes, as evidenced by its negligible influence on all of the fluorescence properties investigated (Figure S4).

The transfer of bacteriorhodopsin or cytochrome  $b_6f$  complex from hydrogenated detergents into an  $F_6OM$  analogue carrying an additional  $CH_2$  group enhances the stability and activity of both proteins.<sup>[34]</sup> This effect requires self-assembly of the fluorinated surfactant to form a membrane-mimetic environment but does not necessitate lipophilicity or detergency. To exemplify how the latter can be exploited for



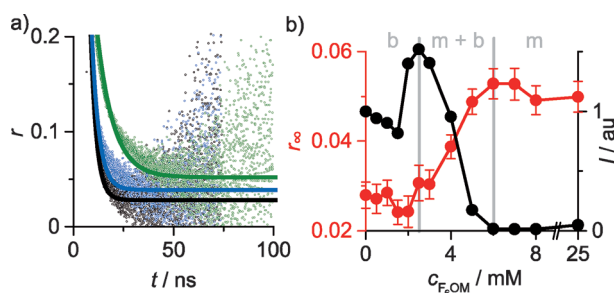


**Figure 5.** Effects of  $F_6OM$  on membrane order as monitored by time-resolved fluorescence anisotropy. a) Representative decays of fluorescence anisotropy  $r$  for  $3.33 \mu M$  DPH in  $2 mM$  POPC LUVs in the absence (black) or presence of  $4 mM$  (blue) or  $10 mM$  (green)  $F_6OM$ . Monoexponential fits (solid lines) yielded limiting anisotropies as asymptotic values. b) Limiting DPH anisotropy ( $r_\infty$ ; red) and  $90^\circ$  light scattering intensity ( $I$ ; black) of  $2 mM$  POPC LUVs as functions of  $F_6OM$  concentration. Gray lines indicate phase boundaries derived from  $I$ , and error bars represent 95% confidence intervals. Each sample was incubated at  $60^\circ C$  for 30 min to ensure equilibration before measurements were performed at  $20^\circ C$ .

membrane-protein applications, we compared the effects of  $F_6OM$  and  $F_6OPC$  on the refolding of outer membrane phospholipase A (OmpLA) to generate enzymatically active proteoliposomes. OmpLA is an excellent model membrane protein for folding studies;<sup>[35]</sup> without chemical or molecular chaperones, however, its urea-unfolded form cannot refold into LUVs composed of long-chain phospholipids.<sup>[36]</sup> By using gel-shift densitometry (Figure 6a) and a colorimetric phospholipase assay<sup>[37]</sup> (Figure S5), we found that the fluorinated detergent  $F_6OM$  could chaperone the functional refolding of OmpLA into POPC LUVs in a concentration-dependent manner without the need for micellar structures (Figure 6b). It outperformed the nondetergent  $F_6OPC$ , which had a significant but moderate effect only in micellar form, a result consistent with a previous report.<sup>[20]</sup>

The lipophobicity of fluorinated surfactants has made them popular for tasks such as the controlled delivery of membrane proteins to preformed lipid bilayers<sup>[20,21]</sup> but has

hampered their application in situations where detergent-like activity is desirable or even essential. Our findings demonstrate that fluorination and detergency are not mutually exclusive and that a fluorinated detergent can aid the functional refolding of a membrane protein under conditions where gentle membrane interactions prove superior to the inertness of lipophobic fluorinated surfactants. While the determining properties await to be elucidated through systematic structure–activity relationship (SAR) studies, the results presented herein suggest that headgroup chemistry can be exploited to tune the balance of lipophobicity versus detergency, thus rendering fluorinated surfactants amenable to a broad range of new applications.

**Keywords:** biomembranes · liposomes · micelles · proteins · surfactants

**How to cite:** *Angew. Chem. Int. Ed.* **2015**, *54*, 5069–5073  
*Angew. Chem.* **2015**, *127*, 5158–5162

- [1] M. Le Maire, P. Champeil, J. V. Møller, *Biochim. Biophys. Acta Biomembr.* **2000**, *1508*, 86–111.
- [2] G. G. Privé, *Methods* **2007**, *41*, 388–397.
- [3] J. L. Rigaud, D. Lévy, *Methods Enzymol.* **2003**, *372*, 65–86.
- [4] N. Jahnke, O. O. Krylova, T. Hoomann, C. Vargas, S. Fiedler, P. Pohl, S. Keller, *Anal. Chem.* **2014**, *86*, 920–927.
- [5] N. Bordag, S. Keller, *Chem. Phys. Lipids* **2010**, *163*, 1–26.
- [6] S. Fiedler, J. Broecker, S. Keller, *Cell. Mol. Life Sci.* **2010**, *67*, 1779–1798.
- [7] J. L. Popot, *Annu. Rev. Biochem.* **2010**, *79*, 737–775.
- [8] A. Nath, W. M. Atkins, S. G. Sligar, *Biochemistry* **2007**, *46*, 2059–2069.
- [9] D. J. K. Swainsbury, S. Scheidelaar, R. van Grondelle, J. A. Killian, M. R. Jones, *Angew. Chem. Int. Ed.* **2014**, *53*, 11803–11807; *Angew. Chem.* **2014**, *126*, 11997–12001.
- [10] J. L. Popot, T. Althoff, D. Bagnard, J. L. Banères, P. Bazzacco, E. Billon-Denis, L. J. Catoire, P. Champeil, D. Charvolin, M. J. Cocco, et al., *Annu. Rev. Biophys.* **2011**, *40*, 379–408.
- [11] P. S. Chae, A. C. Kruse, K. Gotfryd, R. R. Rana, K. H. Cho, S. G. F. Rasmussen, H. E. Bae, R. Chandra, U. Gether, L. Guan, B. K. Kobilka, C. J. Loland, B. Byrne, S. H. Gellman, *Chem. Eur. J.* **2013**, *19*, 15645–15651.

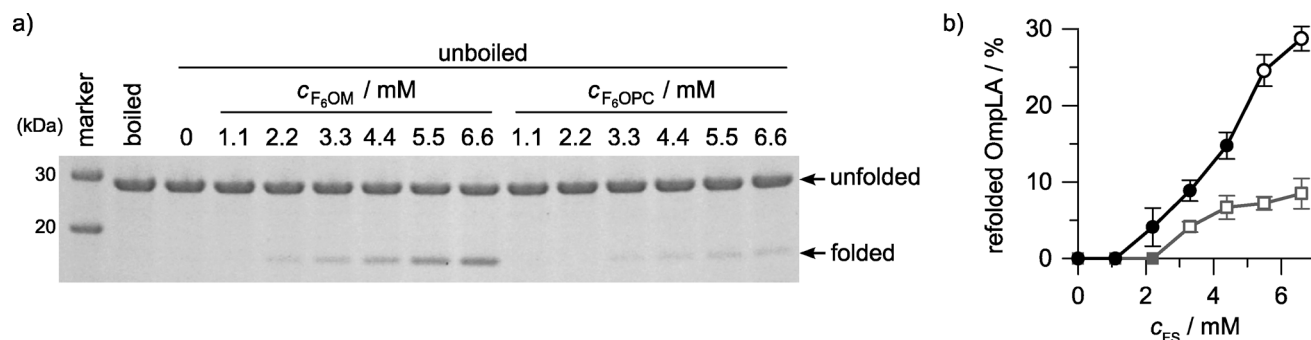


**Figure 6.** Refolding of OmpLA into POPC vesicles in the presence of fluorinated surfactants. a) Sodium dodecyl sulfate (SDS) polyacrylamide gel of OmpLA refolded from  $8 M$  urea into  $4 mM$  POPC LUVs and various concentrations of  $F_6OM$  or  $F_6OPC$ . As a control (second lane), OmpLA was boiled at  $97^\circ C$  for 10 min. b) Fraction of refolded OmpLA versus concentration of fluorinated surfactant ( $c_{FS}$ ), namely,  $F_6OM$  (black) or  $F_6OPC$  (gray), as obtained by densitometric quantification of gels such as the one in (a). For both  $F_6OM$  and  $F_6OPC$ ,  $c_{FS}$  was increased from the submicellar range featuring only bilayers (closed symbols) into the coexistence range containing bilayers and micelles (open symbols), as inferred from the phase diagram (Figure 3b) and demicellization experiments (Figure S2c, d and Figure S3c, d), respectively. Error bars indicate standard deviations from three independent experiments.

- [12] E. Chabaud, P. Barthélémy, N. Mora, J. L. Popot, B. Pucci, *Biochimie* **1998**, *80*, 515–530.
- [13] C. Breyton, E. Chabaud, Y. Chaudier, B. Pucci, J. L. Popot, *FEBS Lett.* **2004**, *564*, 312–318.
- [14] G. Durand, M. Abela, C. Ebel, C. Breyton in *Membrane Proteins Production for Structural Analysis*, (Ed.: I. Mus-Veteau), Springer, Heidelberg, **2014**, pp. 205–251.
- [15] C. Der Mardirossian, M. P. Krafft, T. Gulik-Krzywicki, M. le Maire, F. Lederer, *Biochimie* **1998**, *80*, 531–541.
- [16] P. Barthélémy, V. Tomao, J. Selb, Y. Chaudier, B. Pucci, *Langmuir* **2002**, *18*, 2557–2563.
- [17] S. S. Palchevskyy, Y. O. Posokhov, B. Olivier, J. L. Popot, B. Pucci, A. S. Ladokhin, *Biochemistry* **2006**, *45*, 2629–2635.
- [18] M. V. Rodnin, Y. O. Posokhov, C. Contino-Pépin, J. Brettmann, A. Kyrychenko, S. S. Palchevskyy, B. Pucci, A. S. Ladokhin, *Biophys. J.* **2008**, *94*, 4348–4357.
- [19] F. H. Shepherd, A. Holzenburg, *Anal. Biochem.* **1995**, *224*, 21–27.
- [20] P. Raychaudhuri, Q. Li, A. Mason, E. Mikhailova, A. J. Heron, H. Bayley, *Biochemistry* **2011**, *50*, 1599–1606.
- [21] A. Kyrychenko, M. V. Rodnin, M. Vargas-Urbe, S. K. Sharma, G. Durand, B. Pucci, J. L. Popot, A. S. Ladokhin, *Biochim. Biophys. Acta Biomembr.* **2012**, *1818*, 1006–1012.
- [22] D. Stoddart, M. Ayub, L. Hofler, P. Raychaudhuri, J. W. Klingelhoefer, G. Maglia, A. Heron, H. Bayley, *Proc. Natl. Acad. Sci. USA* **2014**, *111*, 2425–2430.
- [23] M. P. Krafft, F. Giulieri, J. G. Riess, *Angew. Chem. Int. Ed.* **1993**, *32*, 741–743; *Angew. Chem.* **1993**, *105*, 783–785.
- [24] J. Broecker, S. Keller, *Langmuir* **2013**, *29*, 8502–8510.
- [25] S. Keller, H. Heerklotz, N. Jahnke, A. Blume, *Biophys. J.* **2006**, *90*, 4509–4521.
- [26] H. Heerklotz, A. D. Tsamaloukas, S. Keller, *Nat. Protoc.* **2009**, *4*, 686–697.
- [27] S. Keller, I. Sauer, H. Strauss, K. Gast, M. Dathe, M. Bienert, *Angew. Chem. Int. Ed.* **2005**, *44*, 5252–5255; *Angew. Chem.* **2005**, *117*, 5386–5389.
- [28] M. Roux, P. Champeil, *FEBS Lett.* **1984**, *171*, 169–172.
- [29] S. Keller, H. Heerklotz, A. Blume, *J. Am. Chem. Soc.* **2006**, *128*, 1279–1286.
- [30] A. D. Tsamaloukas, S. Keller, H. Heerklotz, *Nat. Protoc.* **2007**, *2*, 695–704.
- [31] J. R. Lakowicz, *Principles of Fluorescence Spectroscopy*, Springer, Boston, **2006**.
- [32] M. Shinitzky, Y. Barenholz, *J. Biol. Chem.* **1974**, *249*, 2652–2657.
- [33] M. Nazari, M. Kurdi, H. Heerklotz, *Biophys. J.* **2012**, *102*, 498–506.
- [34] A. Polidori, M. Presset, F. Lebaupain, B. Ameduri, J. L. Popot, C. Breyton, B. Pucci, *Bioorg. Med. Chem. Lett.* **2006**, *16*, 5827–5831.
- [35] C. P. Moon, K. G. Fleming, *Proc. Natl. Acad. Sci. USA* **2011**, *108*, 10174–10177.
- [36] N. K. Burgess, T. P. Dao, A. M. Stanley, K. G. Fleming, *J. Biol. Chem.* **2008**, *283*, 26748–26758.
- [37] A. J. Aarsman, L. van Deenen, H. van den Bosch, *Bioorg. Chem.* **1976**, *5*, 241–253.

Received: December 24, 2014

Revised: January 22, 2015

Published online: March 9, 2015